the FEBS Journal

# The gene *carD* encodes the aldehyde dehydrogenase responsible for neurosporaxanthin biosynthesis in *Fusarium fujikuroi*

Violeta Díaz-Sánchez[1], Alejandro F. Estrada[1,*], Danika Trautmann[2], Salim Al-Babili[2] and Javier Avalos[1]

1 Departamento de Genética, Facultad de Biología, Universidad de Sevilla, Spain
2 Faculty of Biology, Albert-Ludwigs University of Freiburg, Germany

**Keywords**
apocarotenoids; carotenogenesis; *carS* mutants; light regulation; β-apo-4′-carotenal

**Correspondence**
J. Avalos, Departamento de Genética, Universidad de Sevilla, Apartado 1095, E–41080 Sevilla, Spain
Fax: +34 954557104
Tel: +34 954557110
E-mail: avalos@us.es

***Present address**
Growth & Development, Biozentrum, University of Basel, Klingelbergstrasse 50/70, CH-4056 Basel, Switzerland

(Received 13 May 2011, revised 17 June 2011, accepted 8 July 2011)

doi:10.1111/j.1742-4658.2011.08242.x

Neurosporaxanthin (β-apo-4′-carotenoic acid) biosynthesis has been studied in detail in the fungus *Fusarium fujikuroi*. The genes and enzymes for this biosynthetic pathway are known until the last enzymatic step, the oxidation of the aldehyde group of its precursor, β-apo-4′-carotenal. On the basis of sequence homology to *Neurospora crassa* YLO-1, which mediates the formation of apo-4′-lycopenoic acid from the corresponding aldehyde substrate, we cloned the *carD* gene of *F. fujikuroi* and investigated the activity of the encoded enzyme. *In vitro* assays performed with heterologously expressed protein showed the formation of neurosporaxanthin and other apocarotenoid acids from the corresponding apocarotenals. To confirm this function *in vivo*, we generated an *Escherichia coli* strain producing β-apo-4′-carotenal, which was converted into neurosporaxanthin upon expression of *carD*. Moreover, the *carD* function was substantiated by its targeted disruption in a *F. fujikuroi* carotenoid-overproducing strain, which resulted in the loss of neurosporaxanthin and the accumulation of β-apo-4′-carotenal, its derivative β-apo-4′-carotenol, and minor amounts of other carotenoids. Intermediates accumulated in the Δ*carD* mutant suggest that the reactions leading to neurosporaxanthin in *Neurospora* and *Fusarium* are different in their order. In contrast to *ylo-1* in *N. crassa*, *carD* mRNA content is enhanced by light, but to a lesser extent than other enzymatic genes of the *F. fujikuroi* carotenoid pathway. Furthermore, *carD* mRNA levels were higher in carotenoid-overproducing mutants, supporting a functional role for CarD in *F. fujikuroi* carotenogenesis. With the genetic and biochemical characterization of CarD, the whole neurosporaxanthin biosynthetic pathway of *F. fujikuroi* has been established.

**Database**
The *carD* gene sequence has been deposited in the EMBL Data Bank under accession number FR850689

## Introduction

Carotenoids are tetraterpenoid pigments produced by photosynthetic organisms as well as many bacteria and fungi [1]. Carotenoids are essential in plants, where they are involved in photosystem assembly, light harvesting, photoprotection, quenching, and photomorphogenesis [2]. Carotenoids also have relevant functions in animals, primarily as precursors of retinal and retinoic acid, which are, respectively, involved in

**Abbreviations**
ALDH, aldehyde dehdrogenase; TM, transmembrane.

vision and morphogenesis [3]. Generally, animals are unable to produce these pigments *de novo*, and therefore have to obtain them from dietary sources. In contrast, carotenoid biosynthetic pathways are present in many nonphotosynthetic microorganisms, e.g. filamentous fungi [4]. Moreover, some fungi, such as *Blakeslea trispora* and *Xanthophyllomyces dendrorhous*, are employed for biotechnological carotenoid production [5]. In addition, fungal species such as the ascomycete *Fusarium fujikuroi* (*Gibberella fujikuroi* mating population C) have been particularly convenient organisms for the investigation of carotenoid biosynthesis [6].

The major carotenoid product in *F. fujikuroi* is neurosporaxanthin (β-apo-4′-carotenoic acid), a carboxylic xanthophyll formerly identified in *Neurospora crassa* [7]. Like other carotenoid biosynthetic pathways, neurosporaxanthin biosynthesis (Fig. 1) starts with the formation of the colorless precursor phytoene through the condensation of two molecules of geranylgeranyl diphosphate, a reaction achieved by the phytoene synthase activity of the bifunctional enzyme CarRA [8]. Four desaturations, catalyzed by the phytoene dehydrogenase CarB [9,10], and a terminal cyclization, attributed to the cyclase domain of CarRA, lead to γ-carotene, which is further desaturated by CarB to yield torulene. This reddish carotene is usually not accumulated, but cleaved by the oxygenase CarT [11], to produce β-apo-4′-carotenal. A final oxidation step is needed to convert this aldehyde into the acidic neurosporaxanthin, but the responsible gene of *F. fujikuroi* has not yet been identified. As a parallel route, γ-carotene can be subjected to a second CarRA cyclization reaction leading to β-carotene, which can be symmetrically cleaved by the oxygenase CarX into two molecules of retinal [12], the presumptive chromophore of the rhodopsins CarO [13] and OpsA [14].

The synthesis of neurosporaxanthin in *F. fujikuroi* is stimulated by light [15,16], and derepressed in the dark in the *carS* mutants, which exhibit a deep orange pigmentation irrespective of the culture conditions [15,17]. The genes needed for the synthesis of β-carotene and retinal, *carRA*, *carB*, and *carX*, are clustered with one of the rhodopsin genes, *carO*, in the *F. fujikuroi* genome, whereas the gene needed for torulene cleavage, *carT*, is physically unlinked. Regulation by light and *carS* repression are achieved on gene expression of the five *car* genes: their respective mRNA levels are very low in the dark, and increase rapidly upon illumination; however, *car* mRNA levels are high in the *carS* mutants, either in the light or in the dark [11,13,18].

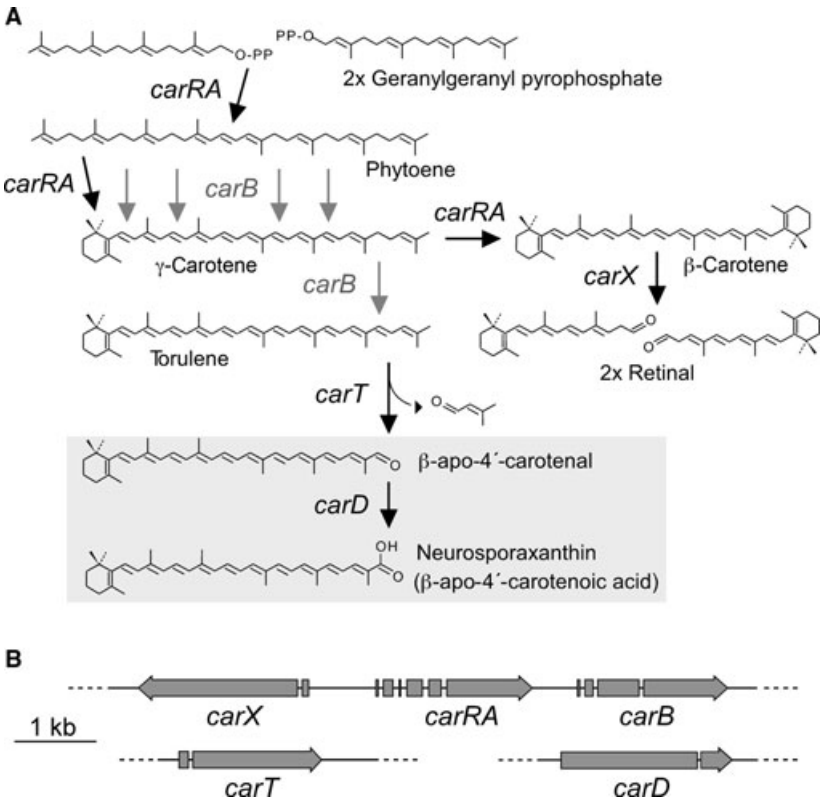


**Fig. 1.** Genes and reactions of carotenoid metabolism in *F. fujikuroi*. (A) Neurosporaxanthin and retinal biosynthetic pathways. Arrows point to chemical changes to the precursor molecule introduced by the indicated enzyme. Desaturations achieved by CarB are indicated in gray for better distinction from CarRA cyclization. Attribution of CarD activity to the shaded reaction is based on data from this work. (B) Genomic organization of enzymatic *car* genes in *F. fujikuroi*. *carT* and *carD* are unlinked to the *car* cluster. The gaps indicate introns.

The genes responsible for light and *carS* transcriptional regulation have not yet been identified. However, targeted mutation experiments have shown that the major photoreceptor is not a White Collar protein, as found in other fungi [19].

The genes orthologous to *carB*, *carRA* and *carT* of *F. fujikuroi* were formerly investigated in *N. crassa* (*al-1* [20], *al-2* [21,22], and *cao-2* [23], respectively). Recently, we identified in this fungus the gene *ylo-1* [24], which is responsible for the aldehyde oxidation step in neurosporaxanthin formation, and showed the ability of the encoded enzyme to convert 4-apocarotenal into this xanthophyll [24]. However, a combination of mutant analysis and enzymatic studies suggested that the pathway proceeds via the oxidation of apo-4′-lycopenal to apo-4′-lycopenoic acid, which is then converted by the cyclase activity of the bifunctional enzyme AL-2 into the cyclic isomer neurosporaxanthin [25]. The goal of this work was to identify and characterize the YLO-1 ortholog, termed CarD, responsible for the final step in neurosporaxanthin biosynthesis in *F. fujikuroi*, which is predicted to be the oxidation of the aldehyde group of β-apo-4′-carotenal. On the basis of sequence homology to *ylo-1*, we identified the *carD* gene and demonstrated, with genetic and biochemical approaches, that the encoded polypeptide carries out the last enzymatic reaction for neurosporaxanthin biosynthesis in *F. fujikuroi*.

## Results

### Identification of *carD*

BLAST analysis of YLO-1 against the genome of *Fusarium verticillioides*, which is closely related to *F. fujikuroi*, identified FVEG02675 as the best match, with a size (539 amino acids) very similar to that of YLO-1 (533 amino acids). The alignment between the polypeptide sequences showed a high degree of conservation along the whole sequence, with 283 coincident positions (53% identity). In addition, FVEG02675 is more similar to YLO-1 of *N. crassa* than to any other aldehyde dehdrogenase (ALDH) enzyme encoded in the *F. verticillioides* genome. Therefore, we postulated that the gene encoding FVEG02675 is the *ylo-1* counterpart of *Fusarium*, which we named *carD*. Further sequence comparisons suggested that CarD enzymes are also encoded in the genomes of *Fusarium oxysporum* and *Fusarium graminearum* (FOXG05463 and FGSG09960, with 98% and 87% identity with FVEG02675, and 53% and 51% with YLO-1, respectively).

Taking advantage of the high similarity between the *Fusarium carD* sequences, we cloned and sequenced *carD* of *F. fujikuroi* (accession number FR850689). The gene sequence was used to amplify the corresponding cDNA and determine the encoded protein (CLUSTAL alignment with YLO-1 is shown in Fig. 2).

```
CarD   MAAAGFDYGCQQSSYTIAPLEHTPLDEIAAKVDLVRKTFRSGRTKDMEFRMKQIRKLYWAIV
YLO-1  MAA---------SKVEIAPFEVTPLDAIPAVCSTARATFASHKTKNLQWRLVQLRKLYWALD
       ***         *.  ***:* **** *.*  . .* ** * :**::::*: *:*******:

CarD   DNTELMQDALIKDLRKCKYEAVLAEIDWCKQECIDMVNNMEKWLRDEPVPNVPLQFRAMKHR
YLO-1  DFKASLMAALQQDLRKGGYESDFTEVDWVKNDCLHMINNLETFAKTEKLKDLPVTYSMMNFR
       * .  :  ** :****  **: ::*:** *::*:.*:**:*.: : * : ::*: :  *:.*

CarD   TRFEPLGVVLNIGSFNFPFQLNLPVVIGAIACGNCVVLKASESSPNCAMVLKKIFDESLDPE
YLO-1  VKKEPLGTVLIIGPYNFPIQLVLAPLVGAIGAGCTAVIKPSELTPACAMAMKEMIESRLDRD
       .: ****.** **.:***:** *. ::***..*  .*:*.** :* ***.:*:::::. ** :

CarD   CFTYVNGALPETQLLLEQKFDKICFTGGKAVGKIIAQKAAETLTPVLLELGGLNPAFVTKHA
YLO-1  AFAVVNGGVPETNALMEEKWDKIMFTGSAQVGSIIARKAAETLTPVCLELGGRNPAFVTKKA
       .*: ***.:***: *:*:*:*** ***.  **.***:********* ***** *******:*

CarD   NLKLAARRLLWQKSLNAGQVCMSHNYILVERGVLSQFLGELNNQMRTFFPQGAKNSPDLCRI
YLO-1  NLALAARRLMWGKVLNAGQVCMSHNYVLVDKDVADTFIEFLKIAYKDMFPNGAKASPDLSRI
       ** ******:* * ************:**::.* . *:  *:   : :**:*** ****.**

CarD   VNAGHFNRLKKMLDGTNGKIVLGGSMDESTLFMEPTAVLVDDINDSMMTQEAFGPIFAMMAV
YLO-1  VNARHFNRIKKMLDETKGKIVMGGEMDESELYIEPTAVLVDSLDDPMMQEESFGPIFSIYPV
       *** ****:***** *:****:**.**** *::********.::*.** :*:*****:: .*

CarD   DSLDQAIDIANTVDPTPLSLSAFGSKAENNKILDNVTSGGATCNDAFFHSQIPQSPLGGVGQ
YLO-1  DTLDQALSIANNVHRTPLALMAFGDKSETNRILDEMTSGGACINDSYFHGAVHTVPFGGVGD
       *:****:.***.*. ***:* ***.*:*.*:***::***** **::**. :   *:****:

CarD   SGMGNYHGIYSIRTFSHQRTIAEVPYWADFLFRVRYMPYQWPVMNRMKAVADSKPNFDRNGN
YLO-1  SGWGAYRGKASFDNFTHFRTVSETPTWMDRFLRVRYMPYDWSELRLLQRWTNKKPNFDRQGT
       ** * *:*  *: .*:* **::*.* * * ::********:*. :. ::  ::.******:*.

                        fg:          F    V
CarD   KTKGITYFLALVLGLGSKK-SKGALLRWAVLVVAAAILEAKKGVLSQLLTR 546
YLO-1  VAKGSEYWMWYFLGLGTKGGVKGALMRWLVVVAGYYLSAYMKARRA----- 533
        :**  *::  .****:*   ****:** *:*..  :    *.  :
```

**Fig. 2.** CLUSTALX alignment of CarD from *F. fujikuroi* and YLO-1 from *N. crassa*. The ALDH domain is shaded in gray. The TM domain of YLO-1 is shaded in black, and the equivalent sequence in CarD is boxed. The two amino acid changes found in this protein segment in *F. graminearum* CarD (FGSG09960, abbreviated *fg*) are indicated above.

The *F. fujikuroi* CarD protein is highly similar to the other *Fusarium* CarD counterparts (472 identical positions in a CLUSTAL alignment between the four protein sequences), but contains seven additional amino acids in its N-terminus (underlined in Fig. 2). The ALDH domain of *F. fujikuroi* CarD extends over 450 of the 546 residues predicted, and is followed by a 91-residue C-terminal extension that also occurs in orthologs, including YLO-1 from *N. crassa* (Fig. 2). Despite the high conservation of the polypetide sequences, CarD differs from YLO-1 [24] in the absence of a transmembrane (TM) domain in its C-terminal region, suggesting differences in the type of association of CarD with the membranes, where its substrate is presumably located. Indeed, the prediction software used to identify this structural feature failed to find any TM domain in the equivalent sequence of any of the *Fusarium* CarD enzymes, where only seven of the 18 residues identified as the TM domain in the YLO-1 sequence are conserved.

## Effect of light and carotenoid overproduction on *carD* expression

Given that CarD is predictably involved in carotenoid biosynthesis, its mRNA levels may be expected to exhibit a regulatory pattern similar to those of other *F. fujikuroi* carotenogenic enzymes. To check this hypothesis, the effects of light and *carS* mutations on *carD* mRNA were investigated. As a reference, *carB*, coding for the phytoene desaturase, was analyzed in parallel. As shown in Fig. 3, *carD* mRNA levels increased about three-fold after 30 min of illumination, and decreased thereafter. This pattern was similar to that observed for *carB*, except that the induction of the latter was much higher and reached nearly 100-fold, consistent with former analysis for this gene under similar growth conditions [14].

To analyze the effect of carotenoid deregulation on *carD* expression, four independent *carS* mutants were investigated. Whereas the wild type produced trace amounts of carotenoids in the dark, the *carS* strains accumulated between 0.5 and 1.5 mg of carotenoids per gram of dry weight (inset in Fig. 3). As expected, the *carB* mRNA levels were much higher in the dark in these strains than in the wild type. Confirming its correlation with other carotenogenic enzymes, the amounts of *carD* mRNA were also enhanced in the *carS* mutants, although to a lower extent (about five-fold, as compared with 100-fold for *carB*). In the light, *carD* mRNA levels were also slightly increased in the mutants, but the subsequent photoadaptation observed in the wild type was not apparent in this case. Taken together, the results of these experiments are consistent with an enzymatic role of *carD* in *F. fujikuroi* carotenoid biosynthesis.

## Enzymatic activity of CarD

To investigate the possible function of CarD in *F. fujikuroi* carotenogenesis, *carD* was expressed in *Escherichia coli*, and the enzymatic activity was assayed *in vitro* with crude protein extracts. As demonstrated by HPLC analysis, incubation with β-apo-4′-carotenal resulted in the formation of neurosporaxanthin (Fig. 4A, upper panel), as verified by LC-MS analysis (Fig. 4B).

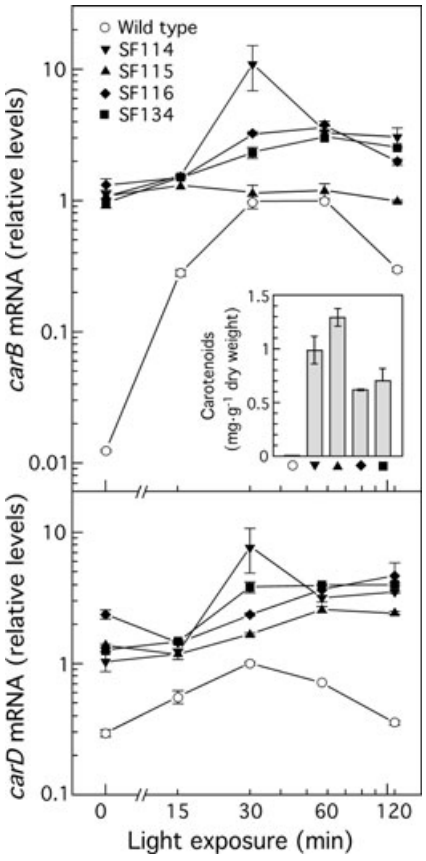


**Fig. 3.** Effect of light on *carB* and *carD* mRNA levels in wild-type and *carS* mutants of *F. fujikuroi*. Real-time RT-PCR analyses of *carB* and *carD* mRNA in total RNA samples of the wild type and the *carS* strains SF114, SF115, SF116, and SF134, grown in the dark or exposed to light for 15 min, 30 min, 1 h, or 2 h. Relative levels are referred to the maximal value determined in the wild type in the light. All data show averages and standard deviations for four measurements from two independent experiments. The inset figure shows the carotenoid amounts in the dark in the five strains investigated.

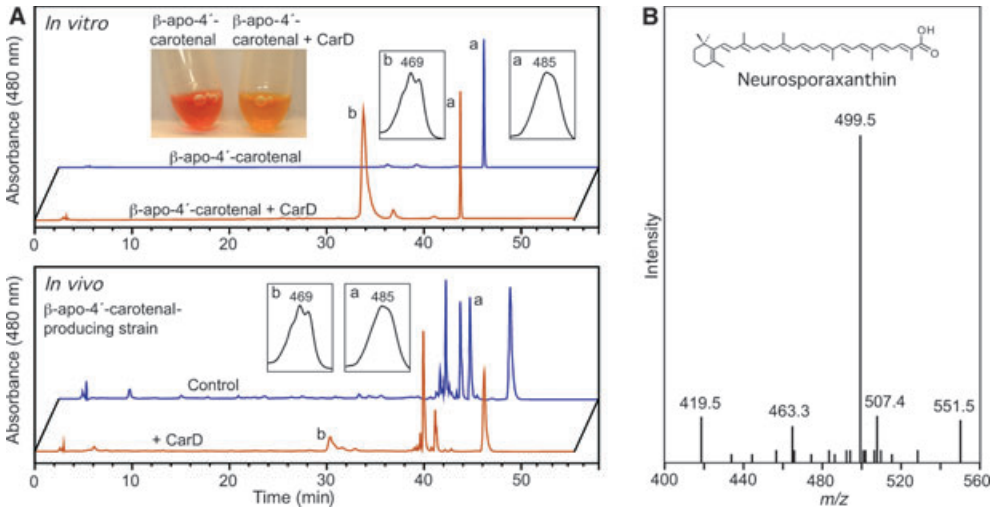


**Fig. 4.** Biochemical assays of CarD activity. (A) Upper panel: HPLC analysis of *in vitro* assays of crude lysate of CarD-expressing cells incubated with β-apo-4′-carotenal (peak a). The generated product (peak b) was identified as neurosporaxanthin by LC-MS analysis (panel B). Oxidation of β-apo-4′-carotenal was accompanied by a change of color (inner picture). Lower panel: *in vivo* test of CarD activity. CarD was expressed in β-apo-4′-carotenal-producing *E. coli* cells. The β-apo-4′-carotenal peak (a) detected among other carotenoids in control cells, which were transformed with pC35 and the void plasmid pThio-BAD, was converted in cells containing pC35 and pThio-CarD into neurosporaxanthin (a). (B) LC-MS analysis of neurosporaxanthin produced in the experiments shown on the left (peak b).

To confirm the CarD activity *in vivo*, we engineered a carotenoid pathway in *E. coli* to lead to the production of β-apo-4′-carotenal. For this purpose, we constructed plasmid pC35, encoding a set of *Neurospora* and *Erwinia* enzymes and the *F. fujikuroi* torulene cleavage oxygenase CarT, a combination enabling accumulation of torulene in *E. coli* for *in vitro* experiments. Indeed, *E. coli* cells transformed with pC35 or with pC35 and the void plasmid pThio/BAD (Fig. 4A, lower panel, control) were shown to accumulate β-apo-4′-carotenal (Fig. 4A, lower panel, control, peak a), besides other pigments.

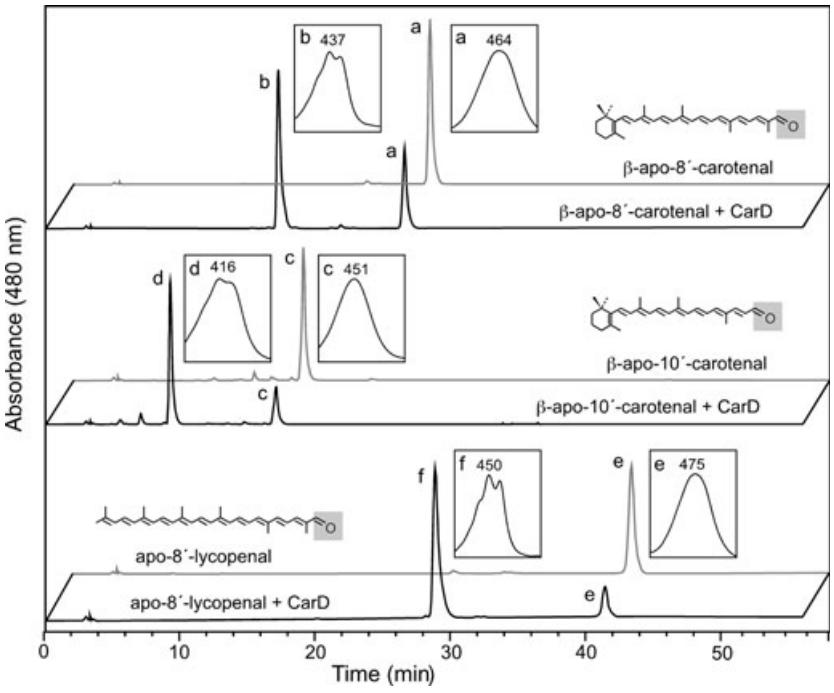


**Fig. 5.** *In vitro* activity of CarD on different apocarotenals. HPLC analyses of *in vitro* assays of crude lysate of CarD-expressing cells incubated with β-apo-8′-carotenal (top), β-apo-10′-carotenal (middle), and apo-8′-lycopenal (bottom). The chromatograms in gray show the corresponding incubations with crude lysate of cells transformed with the void plasmid pThio-BAD. Absorption spectra and maximal absorption wavelengths of the relevant peaks are shown in boxes.

Expression of CarD, encoded in pThio-CarD, in this background led to a reduction in the amount of β-apo-4′-carotenal and the formation of neurosporaxanthin (Fig. 4A, lower panel, peak b).

To check the specificity of the CarD enzymatic activity, crude extracts from *carD*-expressing *E. coli* cells were incubated with shorter apocarotenals, i.e. β-apo-8′-carotenal ($C_{30}$), β-apo-10′-carotenal ($C_{27}$), and β-apo-15′-carotenal ($C_{20}$; retinal), and with the acyclic apocarotenal apo-8′-lycopenal ($C_{30}$). HPLC analyses (Fig. 5) showed the formation of apo-8′-lycopenoic acid, β-apo-8′-carotenoic acid and β-apo-10′-carotenoic acid from the corresponding aldehydes, indicating wide substrate specificity. However, retinal ($C_{20}$) was not converted (data not shown), indicating the requirement for a minimal length of the substrate chain.

## Generation of targeted Δ*carD F. fujikuroi* mutants

Our expression and biochemical analyses suggested that CarD is a candidate for the conversion of β-apo-4′-carotenal to neurosporaxanthin in the *F. fujikuroi* carotenoid pathway (Fig. 1). To obtain genetic evidence for this function, transformation experiments were carried out to obtain null *carD* mutants of *F. fujikuroi* by targeted gene replacement with a hygromycin resistance cassette (Fig. 6A). For better visualization of the effect on carotenogenesis, *carD* replacement was performed in the *carS* strain SF134. After incubation of SF134 protoplasts with plasmid pVIO6, 12 hygromycin-resistant transformants were obtained. All of the transformants exhibited the deep-orange pigmentation, but a detailed visual inspection revealed the formation of orange–yellowish sectors in two of them upon prolonged incubation, suggesting the segregation of a mutated homokaryotic phenotype from heterokaryotic mycelia. As this pigmentation indicated a change in the carotenoid pattern, the orange–yellowish sectors were suspected to harbor the Δ*carD* mutation, and were therefore purified and passed through single uninucleate conidia. These transformant strains were named T3 and T4.

The molecular integrity of *carD* was investigated in T3 and T4 strains, in two nonsectoring transformants, T1 and T2, and in the SF134 original strain. A PCR test showed the absence of the wild-type *carD* allele in T3 and T4 but not in T1 and T2 (Fig. 6B). Southern blot analysis of genomic DNA from these strains, using a probe of the *carD* gene containing deleted and non-deleted sequences, confirmed the expected gene replacement in T3 and T4, but not in T1 and T2 (Fig. 6C), which contained both wild-type and defective alleles. These latter strains probably have ectopically integrated pVIO6 sequences. Therefore, T3 and T4 were chosen for detailed phenotypic characterization.

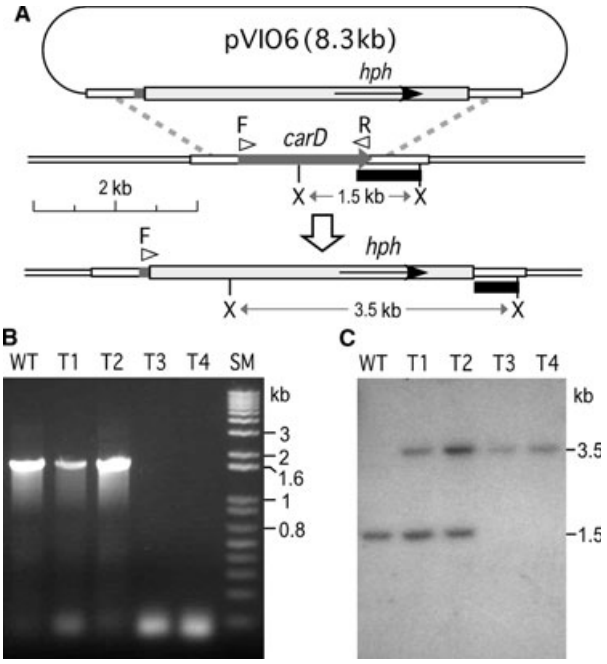


**Fig. 6.** Generation of targeted Δ*carD* mutants in a *carS* background. (A) Schematic representation of the gene replacement event leading to the generation of hygromycin-resistant Δ*carD* transformants. Plasmid pVIO6 contains the *hygR* cassette with the *hph* gene surrounded by 5′ and 3′ *carD* sequences. The recombination events leading to *carD* disruption and the resulting physical map in the generated Δ*carD* mutants are also shown. Open arrowheads indicate forward and reverse primers used in the PCR test of (B). The black bar delimits the probe used in the Southern blot shown in (C). Relevant fragments produced by digestion with *Xho*I are indicated. (B) Detection of wild-type *carD* alleles in the *carS* mutant SF134 and the four transformants described in the text. The picture shows the electrophoretic separation of PCR amplification products obtained with the forward and reverse primers. The 1.6-kb amplification product indicates the presence of the wild-type allele. SM indicates size markers (relevant sizes shown on the right in kilobases). (C) Southern blot of genomic DNA from the wild type (WT) and the four transformants investigated in the PCR analysis, digested with *Xho*I and hybridized with the *carD* probe indicated above.

## Phenotype of Δ*carD* mutants

Comparison of T3 and T4 colonies with those of the preceding SF134 strain confirmed a different color of their mycelia. The difference in color increased with age, as the strains harboring the Δ*carD* mutation acquired a yellowish pigmentation (Fig. 7A, upper picture). For carotenoid analysis, the strains were grown in the dark in low-nitrogen medium, which was formerly reported to allow a higher level of carotenoid

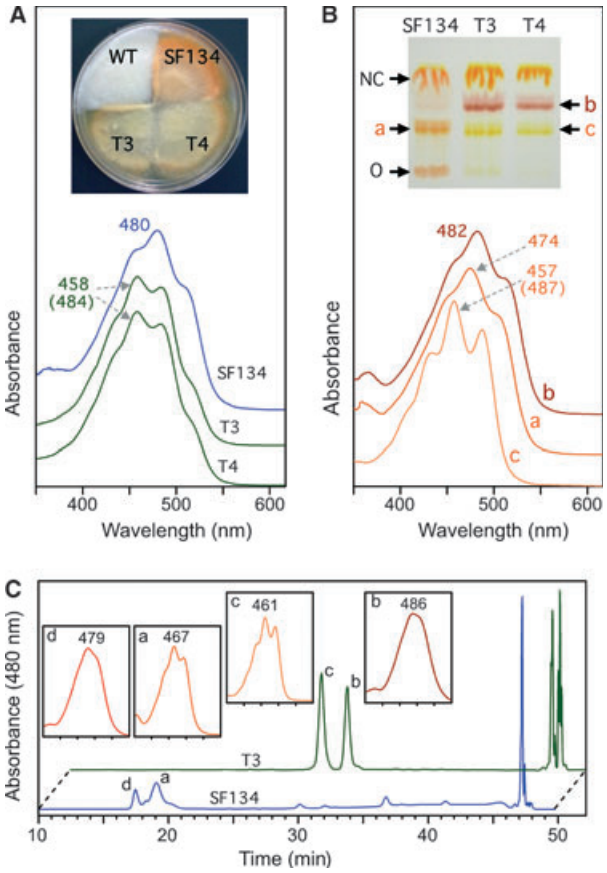


**Fig. 7.** Effect of the Δ*carD* mutation on carotenoid production in a *carS* mutant of *F. fujikuroi*. (A) Absorption spectra of the carotenoids produced by SF134 (blue) and the Δ*carD* mutants T3 and T4 (green) grown in low-nitrogen medium. Wavelengths of maximal absorption peaks are indicated. The upper picture shows colonies of the same strains grown for 2 weeks on minimal medium in the dark. (B) TLC separation of the carotenoid samples shown in (A). Neutral carotenoids (NC) run on the front. O indicates the origin. Bands a, b and c were scraped out and resuspended in hexane for spectrophotometric analysis; their absorption spectra and wavelengths of maximal absorption peaks are shown below. (C) HPLC analyses of the carotenoids produced by SF134 (blue) and the Δ*carD* mutant T3 (green). Absorption spectra and maximal absorption wavelengths of the relevant peaks are shown in boxes.

production [17]. In agreement with the yellowish pigmentation of their mycelia, the absorption spectra of the crude carotenoid samples from T3 and T4 had a different shape and exhibited a maximal absorbance at a shorter wavelength than those from SF134 (Fig. 7A).

Separation of the carotenoids from the three strains on a TLC plate revealed the presence of neutral carotenoids, running in the front (NC in Fig. 7B), and polar carotenoids, running in lower positions. Neurosporaxanthin was found in the SF134 extract (Fig. 7B,a), but not in the T3 and T4 carotenoid samples. Instead, these Δ*carD* mutants had prominent reddish and yellowish bands (Fig. 7B,b,c). The absorption spectrum of the eluted reddish band was very similar to that of neurosporaxanthin, but with an 8-nm shift in its maximal absorption wavelength (482 nm instead of 474 nm). The UV–visible spectrum of the reddish band and its migration pattern on the TLC plate coincided with those of β-apo-4′-carotenal. The position of the yellow band in the TLC chromatogram indicates that it is a polar carotenoid, but its absorption spectrum does not coincide with that of any formerly known carotenoid in *Fusarium*.

The TLC carotenoid pattern for the three strains was confirmed by HPLC. T3 and T4 exhibited identical profiles (results for T3 are displayed in Fig. 7C). The elution chromatogram confirmed the total absence of neurosporaxanthin in the Δ*carD* mutant and the accumulation of two compounds (Fig. 7C, peaks b,c) corresponding to β-apo-4′-carotenal and the TLC-detected yellowish carotenoid (Fig. 7B,b,c). Both compounds were also found in trace amounts in SF134. On the basis of its chromatographic properties, we postulated that the yellowish carotenoid is the alcohol derivative of β-apo-4′-carotenal. As a chemical demonstration, a sample of β-apo-4′-carotenal was eluted from the TLC plate (Fig. 7B,b) and reduced by treatment with $NaBH_4$. The reddish pigmentation rapidly turned yellow, and the resulting product showed the same elution and absorption spectrum as the yellowish carotenoid eluted from the TLC plate (Fig. 8). Thus, we concluded that the yellowish carotenoid is β-apo-8′-carotenol.

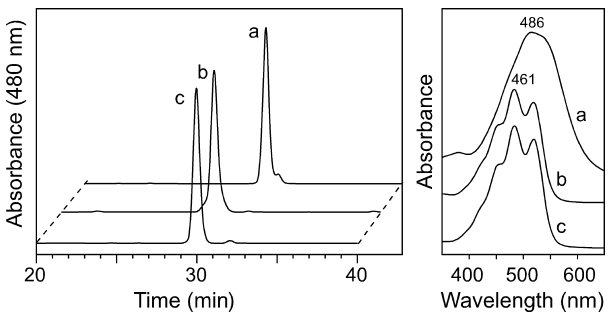


**Fig. 8.** Chemical reduction of the aldehyde group of β-apo-4′-carotenal to produce β-apo-4′-carotenol. A β-apo-4′-carotenal sample was scraped out from the TLC separation of the Δ*carD* mutant (Fig. 7B, sample b), treated with $NaBH_4$, and analyzed by HPLC. The HPLC profile (left panel) and absorption spectrum (right panel) of the carotenoid product (b) were identical to those of the yellow carotenoid produced by the Δ*carD* mutant T3 (c) and different from those of the untreated β-apo-4′-carotenal sample (a).

A detailed analysis of the elution chromatogram for the neutral carotenoids (47–48 min in Fig. 7C; amplified chromatogram and peak spectra in Fig. S1) is consistent with the accumulation of torulene and γ-carotene in both SF134 and Δ*carD* mutants. However, three additional peaks eluting around 48 min were apparent in the chromatogram for Δ*carD* but not in that for SF134. The three peaks showed a similar shape and identical maximal absorption wavelength (461 nm) as β-apo-4′-carotenol (Fig. 7C, peak b), indicating that they might be fatty acid esters of β-apo-4′-carotenol.

## Discussion

In this work, *carD*, encoding the ALDH responsible for neurosporaxanthin biosynthesis in *F. fujikuroi*, has been identified and characterized. Two different experimental approaches, i.e. the incubation of heterologously expressed CarD with β-apo-4′-carotenal *in vitro*, and the expression of *carD* in a β-apo-4′-carotenal-producing *E. coli* strain *in vivo*, allowed us to demonstrate the activity of CarD in converting β-apo-4′-carotenal to neurosporaxanthin. In further support of this, the targeted mutation of *carD* in a carotenoid-overproducing strain led to the loss of neurosporaxanthin biosynthetic capacity and the accumulation of the precursor β-apo-4′-carotenal and its corresponding alcohol β-apo-4′-carotenol. In addition, the occurrence of the same pathway and the same genes and *car* gene cluster in other *Fusarium/Gibberella* species (e.g. *Gibberella zeae* [26], and unpublished analyses of available *Fusarium* genome databases) strongly suggests the generalization of this functional attribution in this taxonomic group.

Our *in vitro* incubations of CarD with substrates other than β-apo-4′-carotenal revealed a wide substrate specificity. For instance, the conversion of apo-8′-lycopenal demonstrates that the occurrence of a β-ionone ring in the substrate is not compulsory for the enzymatic activity. In addition, CarD is able to oxidize the aldehyde group of different apocarotenals, as shown for β-apo-10′-carotenal ($C_{30}$) and β-apo-8′-carotenal ($C_{27}$), besides the presumed natural substrate, β-apo-4′-carotenal ($C_{35}$). However, the lack of activity on retinal ($C_{20}$) indicates a minimal length requirement for the aliphatic chain of the substrate. Retinal is an apocarotenal that is predicted to occur in *F. fujikuroi* [12], where it is presumably needed for opsin photoactivity. The partial deregulation of carotenoid biosynthesis found in the absence of retinal production [18] could be attributed to a regulatory function of retinal, or a derivative molecule, such as retinoic acid. The inability of CarD to produce retinoic acid from retinal apparently excludes this enzyme for this reaction. However, our *in vitro* data do not allow us to rule out this possible function *in vivo*. Currently, a screen of ALDHs is being performed in *Fusarium*, in order to identify an enzyme forming retinoic acid.

The phenotype produced through deletion of *carD* in *F. fujikuroi* is reminiscent of that of the ortholog *ylo-1* in *N. crassa* in the color shift to a yellowish pigmentation and in the absence of neurosporaxanthin. However, the two species employ different orders in the sequence of reactions leading to this major pigment. In contrast to what was seen in the *F. fujikuroi* Δ*carD* mutant, β-apo-4′-carotenal was undetectable in the *N. crassa ylo-1* mutant grown under optimal conditions for neurosporaxanthin production. Instead, the *ylo-1* mutant accumulated a mixture of lycopene, apo-4′-lycopenal, and apo-4′-lycopenol, suggesting that the cyclization of apo-4′-lycopenoic acid is the last step in the neurosporaxanthin pathway, taking place after the oxidative reactions in this fungus [25].

The presence of apo-4′-lycopenol in the *ylo-1* strain parallels the presence of β-apo-4′-carotenol in the Δ*carD* mutant of *F. fujikuroi*. In both cases, the aldehyde groups of the apocarotenal intermediates are reduced to alcohol groups, probably to avoid an accumulation of aldehydes that may have adverse effects, e.g. through formation of Schiff bases with lysines. Indeed, the Δ*carD* and *ylo-1* strains do not show retarded growth when compared with the corresponding wild-type strains. Xanthophylls have higher antioxidant activity than nonoxygenated carotenoids [27], but the potential antioxidant activity of neurosporaxanthin has not been assayed. Experiments in progress to evaluate a possible protective role of neurosporaxanthin against oxidative stress in *F. fujikuroi* will be extended to Δ*carD* strains, to determine the putative advantage of the carboxylic group over its aldehyde or alcohol versions.

In regulation terms, *carD* is like other *car* genes of *F. fujikuroi* in the transient light induction of its mRNA levels [13,14]. However, the three-fold induction was modest as compared with that observed for the other *car* genes (100-fold for *carB* in the same RNA samples), and contrasts with the total absence of light induction of *ylo-1* mRNA levels in *N. crassa* [24]. The availability of transcriptionally derepressed carotenoid-overproducing strains (*carS*) in *F. fujikuroi*, unknown in *N. crassa*, is valuable for evaluation of the regulatory connection of *carD* with carotenogenesis. The *carS* mutants are deeply pigmented, accumulate high amounts of carotenoids under any conditions tested [10,15,17,28], and show enhanced carotenogenic

activity *in vitro* [29]. Correspondingly, they exhibit high mRNA levels for the enzymatic genes either under light or in the dark [10,11,13,17,18]. The enhanced *carD* mRNA levels in four independent *carS* mutants supports coordinated regulation of this gene with others involved in the carotenoid pathway.

Apart from a presumed antioxidative impact, the biological function(s) of neurosporaxanthin in *F. fujikuroi* or *N. crassa* and the possible implications of its carboxylic group for its interactions in the membranes are still to be elucidated. Except for the albino phenotype, mutants lacking carotenoids exhibit normal growth and morphology under laboratory conditions, as do *ylo-1* and Δ*carD* mutants. The carotenoid amounts in wild-type *F. fujikuroi* in the light are modest, about 0.1 $mg \cdot g^{-1}$ dry weight, but the *carS* mutants accumulate $\sim$ 10 times more, without any apparent phenotypic consequence, except for the enhanced pigmentation and other changes in secondary metabolite production [17]. The carotenoids detected in the Δ*carD* mutant suggest significant reactivity of the aldehyde group of the late intermediate of the pathway, β-apo-4′-carotenal, which is partially reduced to alcohol. Further modifications may also occur, as indicated by the 461-nm-absorbing carotenoids detected in the Δ*carD* mutant, whose elution times in the HPLC profiles are consistent with fatty acid esters of different chain lengths. Neurosporaxanthin is apparently more stable than β-apo-4′-carotenal, as judged by the apparent lack of presumptive derivatives in the HPLC profiles of the parent strain. However, the carboxy group is subject to esterification reactions in other species, yielding a methyl ester derivative in another neurosporaxanthin-producing ascomycete, *Verticillium agaricinum* [30], and a glycosyl ester in a marine *Fusarium* species [31].

The identification of *carD* fills the last gap in our knowledge of the enzymes needed for neurosporaxanthin biosynthesis in *F. fujikuroi*, a fungus that shares the accumulation of this xanthophyll with *N. crassa*. The similarity between the carotenogenic enzymes from these two species suggests a common origin from an ascomycete ancestor, which might also be the ancestor of *V. agaricinum*, the third fungus in which this uncommon carotenoid has been identified [32]. c*arD* is unlinked to the *car* cluster of *F. fujikuroi*, which groups the genes needed to produce retinal and the rhodopsin protein, CarO. The torulene-cleaving oxygenase CarT was postulated to be a later acquisition, allowing a torulene-producing organism to produce β-apo-4′-carotenal. Thus, CarD was likely to have an enzymatic activity that was subsequently recruited to produce the carboxylic version of this apocarotenoid.

## Experimental procedures

### Strains and growth conditions

FKMC1995 [33] is a wild-type strain of *F. fujikuroi* (formerly, *G. fujikuroi* mating population C [34]). SF134, SF114, SF115 and SF116 are carotenoid-overproducing strains obtained by exposure of FKMC1995 conidia to *N*-methyl-*N*′-nitro-*N*′-nitrosoguanidine [35].

Unless otherwise stated, experiments were performed on DG minimal medium [35], with L-asparagine instead of sodium nitrate as nitrogen source (called here DGasn medium). For carotenoid analyses of Δ*carD* mutants, incubations were performed in 500-mL Erlenmeyer flasks with 250 mL of culture medium, inoculated with $10^6$ conidia, and grown at 30 °C in the dark on an orbital shaker at 150 r.p.m. For higher carotenoid production, the strains were grown in low-nitrogen medium [17]. For expression analyses, 140-mm-wide Petri dishes containing 80 mL of medium were inoculated with $10^6$ conidia and incubated at 30 °C in the dark for 3 days. When indicated, the dish was illuminated under 25 $W \cdot m^{-2}$ for different times before mycelia filtration. For carotenoid analysis of the strains used in the expression experiments, incubations were performed for 7 days in the dark at 22 °C. For large-scale DNA preparation, 250-mL Erlenmeyer flasks containing 50 mL of medium were inoculated with $10^8$ conidia and incubated for 2 days at 30 °C before filtration. In all cases, the mycelial samples were separated from the medium with filter paper, frozen (using liquid nitrogen when used for RNA samples), and stored at −80 °C. When required, the medium was supplemented with 100 μg hygromycin·$mL^{-1}$. For *in vitro* and *in vivo* assays, BL21-accumulating and 4-apo-carotenal-accumulating *E. coli* strains were incubated in 2 × YT medium (16 $g \cdot L^{-1}$ tryptone, 10 $g \cdot L^{-1}$ yeast extract, and 5 $g \cdot L^{-1}$ NaCl) and LB (10 $g \cdot L^{-1}$ tryptone, 5 $g \cdot L^{-1}$ yeast extract, and 5 $g \cdot L^{-1}$ NaCl), respectively.

### Cloning of *carD*

On the basis of the sequence conservation between the *F. fujikuroi* genome and those of other *Fusarium* species, two sets of primers were chosen from the *F. verticillioides* FVEG02675 gene sequence conserved in the *F. oxysporum* counterpart to clone two overlapping DNA segments from the *F. fujikuroi* homologous region. Each primer set contained one primer annealing within the gene and another either upstream (5′-GAGCGGGGGTTAGGAGAGG-3′/5′-TCATCGAGAGGCGTGTGCTC-3′) or downstream (5′-GCGCTCTTCTCAGGTGGGC-3′/5′-CTTCTCTTGC TGGTACTCTCAC-3′) in the noncoding regions. The resulting PCR products were cloned in pGEM-T Easy (Promega, Mannheim, Germany), with *F. fujikuroi* genomic DNA as a template, and sequenced to confirm their identities. To reduce the chance of point mutations, all PCR

reactions were carried out with the Expand High Fidelity PCR System (Roche). The sequences of both DNA strands from each segment were determined from at least two independent PCR products. For *in vitro* analysis, the *carD* coding sequence was amplified by PCR, with the primers 5′-ATGGCTGCCAACAATCATCC-3′ and 5′-CGGTGTT AGACCACCGAATC-3′, from cDNA obtained from a total RNA sample of the SF134 strain with the SuperScript III First-Strand System for RT-PCR (Invitrogen, Paisley, UK). The PCR product was cloned into pBAD/THIO-TOPO TA vector (Invitrogen), yielding pThio-carD. The inserted *carD* cDNA was sequenced to confirm integrity and orientation.

## Construction of plasmid pC35

In a first approach, a plasmid enabling accumulation of torulene was constructed by introducing *al-2*, encoding the *N. crassa* phytoene synthase/carotene cyclase, into pFarbeR-AL1-ind [25] and driven by the inducible *lac* promoter. For this purpose, a *Not*I–*Xba*I fragment coding for *lac-al2* was excised from pFarbe-R-Al2 (unpublished data), a pFDY297 derivative carrying an *Erwinia* lycopene synthesis cassette, including *CrtE*, *ORF6*, *CrtI*, and *CrtB*, upstream of a *lac-al2* expression cassette, and inserted into the corresponding sites of pFarbeR-AL1-ind, yielding pTorulene. A *ptac–GEX–carY* fragment encoding the *F. fujikuroi* torulene cleavage dioxygenase CarT in fusion with GEX and under the control of the isopropyl thio-β-D-galactoside-inducible *ptac* promoter was then amplified from pGEXYs [11] with the primers 5′-TTTGGCGCGCCATCATAA CGGTTCTGGCAAAT-3′ and 5′-TTCGGCGCGCCTTA AGCAGCTGGCAAATGAATG-3′, both of them carrying an *Asc*I site. The PCR reaction was performed with one unit of Phusion High-Fidelity DNA Polymerase (Finnzymes, Espoo, Finland), according to the instructions of the manufacturer. The obtained fragment was digested with *Asc*I and ligated into *Asc*I-digested pTorulene, to yield p-C35.

## Generation of Δ*carD* mutants

A plasmid was constructed in which most of the *carD* coding sequence was replaced by a hygromycin resistance cassette, containing the *hph* gene. *carD* was obtained by PCR from FKMC1995 genomic DNA with primers 5′-TACC AGTTCAACCCATACTACG-3′ and 5′-CAGCGGGC ATCAACCGTATG-3′. The resulting 2.9-kb DNA product, which included 759 bp and 547 bp of upstream and downstream noncoding sequences, respectively, was cloned into the pGEM-T Easy vector. A reverse PCR reaction was carried out on the resulting plasmid with the primers 5′-CG AAGCTTGATTCGGTGGTCTAACACC-3′ and 5′-CCAG ATCTCCAGTACAGCTTGCGAATC-3′, extended with restriction sites for *Hin*dIII and *Bgl*II, respectively. The resulting 4.6-kb DNA product, which lacks 1509 bp of the 1669-bp *carD* coding sequence, was ligated with a 3.8-kb segment containing the *hph* gene obtained by digestion of vector pAN7-1 [36] with the enzymes *Hin*dIII and *Bgl*II, to yield plasmid pVIO6. The orientation of the inserts was determined by restriction analysis.

To obtain the Δ*carD* mutants, about $10^8$ SF134 protoplasts were isolated according to Prado-Cabrero *et al.* [11] and exposed to *Dra*I-linearized pVIO6, following the transformation protocol described by Proctor *et al.* [37]. The resulting hygromycin-resistant colonies were passed through single conidia, checked for conservation of the hygromycin-resistant phenotype, and analyzed by Southern blot hybridizations, performed as described in [38]. The nylon membrane was probed with a 828-bp segment including the end of the *carD* ORF and a downstream segment (see Fig. 6) obtained by PCR with the primers 5′-CGAAGCTTTGAA CCGAATGAAGGCGGT-3′ and 5′-CAGCGGGCATCA ACCGTATG-3′.

## Expression analyses

Real-time RT-PCR expression analyses were performed on total RNA samples extracted with the RNeasy Plant Mini Kit (Qiagen). Reaction mixtures contained 12 μL of SYBR Green PCR Master Mix 2X (Applied Biosystems, Branchburg, NJ, USA), 0.125 μL of MultiScribe Reverse Transcriptase ($50\ U{\cdot}mL^{-1}$), 0.125 μL of RNase Inhibitor ($10\ U{\cdot}mL^{-1}$), 50 ng of RNA, and 5 mM each primer. The reactions, carried out in 25-μL volumes on an ABI 7500 (Applied Biosystems), consisted of 30 min of retrotranscription at 48 °C, 10 min at 95 °C, and 40 cycles of 95 °C denaturation for 15 s and 60 °C polymerization for 1 min. Dissociation curves were then obtained. The primer sets for detecting *carD* (5′-TGACCTTTGCCGCATCGT-3′/5′-TGGTGCCATCAAGCATCTTC-3′) and *carB* (5′-TCGG TGTCGAGTACCGTCTCT-3′/5′-TGCCTTGCCGGTTGC TT-3′) were designed according to PRIMER EXPRESS v2.0.0 software (Applied Biosystems) and synthesized by StabVida (Oeiras, Portugal). $MgCl_2$ and primer concentrations, and annealing temperatures, were optimized as recommended by the manufacturer. The β-tubulin gene from *F. fujikuroi* (5′-CCGGTGCTGGAAACAACTG-3′/5′-CGAGGACCT GGTCGACAAGT-3′) was used as a control for constitutive expression. Relative gene expression was calculated with the $2^{-\Delta\Delta CT}$ method with SEQUENCE DETECTION software v1.2.2 (Applied Biosystems). Each RT-PCR reaction was performed twice to ensure statistical accuracy.

## Protein expression and *in vitro* assays

The *E. coli* BL21 strain was transformed with pThio-carD; ampicillin-resistant cells were grown at 28 °C up to a $D_{600\ nm}$ of 0.5 and induced with 0.5 mL of 20% arabinose. After incubation for an additional 4 h, cells were

harvested by centrifugation at 12 000 ***g*** for 1 min and resuspended in 50 mM $NaH_2PO_4$, 300 mM NaCl, 1 mg·mL$^{-1}$ lysozyme, 1 mM dithiothreitol, and 0.1% Triton X-100 (v/v) (pH 8.0). After incubation for 30 min on ice, cells were sonicated and centrifuged at 12 000 ***g*** at 4 °C for 30 min, and isolated supernatant was used as crude lysate for *in vitro* assays. To produce micelles, dried substrate was dissolved in 20 μL of 1% Triton X-100 in ethanol (v/v) to yield a final concentration of ~ 500 μM and dried in a vacuum centrifuge. The resulting gel was resuspended in 100 μL of incubation buffer (200 mM pyrophosphate, 200 mM NaCl, pH 7.5, 2 μL of 100 mM $NAD^+$), and 80 μL of crude protein and water were added to give a total volume of 200 μL. Incubations were performed at 28 °C for 30 min, stopped by addition of 1 mL of acetone, extracted with light petroleum/diethyl ether (1 : 4, v/v) and subjected to HPLC analysis.

### *In vivo* analysis

JM 109 *E. coli* cells harboring pC35 were transformed with pThio-carD or pBAD/Thio, and overnight colonies were inoculated into LB medium supplemented with 0.1 mM isopropyl thio-β-D-galactoside and grown at 28 °C to a $D_{600\ nm}$ of 0.5. Expression of CarD was then induced by adding arabinose to a concentration of 0.2% (v/v). After 4 h, cultures were harvested by centrifugation at 12 000 ***g*** for 1 min, and pigments were extracted by dissolving the pellets in 5 mL of acetone, sonication, and centrifugation at 12 000 ***g*** for 10 min. Extraction was repeated, and extracts were combined, dried and subjected to HPLC analysis.

### Carotenoid analyses

Carotenoids were extracted with acetone from lyophilized, sand-ground mycelial samples and dried under vacuum. Total amounts of colored carotenoids were estimated from absorption maxima in hexane, with an average maximal ε (1 mg·mL$^{-1}$·cm$^{-1}$) value of 0.2.

Neutral and polar carotenoids extracted from *in vivo* assays and from SF134 and transformant strains were separated by TLC on silica gel plates developed in light petroleum/diethyl ether/acetone (4 : 1 : 1, v/v/v). The bands corresponding to different carotenoids were scraped out, dissolved in acetone, and subjected to either spectrophotometric, HPLC or LC-MS analyses.

HPLC separations were performed in a Waters System (Waters, Eschborn, Germany) equipped with a photodiode array detector (model 996) and a C30 reverse-phase column (YMC Europe, Schermbeck, Germany) or in a Hewlett Packard 1100 series system (Waldbronn, Germany) equipped with a photodiode array detector and a C30 column (ProntoSIL, 250 × 4.6-mm internal diameter, 5 μm), using solvent systems A (MeOH/t-butylmethyl ether 1 : 1, v/v) and B (MeOH/t-butylmethyl ether/water, 600 : 120 : 120, v/v/v). The column was developed at a flow rate of 1 mL·min$^{-1}$, with a linear gradient from 100% B to 43% B within 45 min, and then to 0% within 1 min, with the final conditions being maintained for another 24 min at a flow rate of 2 mL·min$^{-1}$. LC-MS analyses were performed as described by Estrada *et al.* [24].

### Chemical reduction of β-apo-4′-carotenal

To reduce the aldehyde group of β-apo-4′-carotenal, the corresponding band was scraped out from a TLC plate and dissolved in 2 mL of EtOH. About 10 mg of $NaBH_4$ was added, and the mixture was incubated for 20 min at room temperature. Drops of 1 M HCl were added and mixed carefully, until no bubbles were formed. The reduced carotenoid product was recovered by partition with light petroleum/diethyl ether (1 : 4).

### Protein sequence analyses

Protein alignment was achieved with CLUSTALX 1.83 [39]. The occurrence of TM domains was checked with the SMART architecture research online tool (http://smart.embl.de/, [40]).

## Acknowledgements

This work was supported by the European Union (European Regional Development Fund, ERDF), the Spanish Government (Ministerio de Ciencia y Tecnología, projects BIO2003-01548 and BIO2006-01323), the Andalusian Government (project P07-CVI-02813), and the Deutsche Forschungsgemeinschaft (DFG) (Grant AL892-1-4). We are indebted to P. Beyer for valuable discussions and to D. Maier and D. Scherzinger for skillful technical help. We are grateful to J. Weidner for grammar revision.

## References

1 Britton G, Liaaen-Jensen S & Pfander H (1998) *Carotenoids*. Birkhäuser Verlag, Basel.
2 Cuttriss AJ & Pogson BJ (2006) Carotenoids. In *The Structure and Function of Plastids* (Wise RR & Hoober JK eds), pp. 315–334. Springer, Dordrecht, The Netherlands.
3 von Lintig J (2010) Colors with functions: elucidating the biochemical and molecular basis of carotenoid metabolism. *Annu Rev Nutr* **30**, 35–56.
4 Sandmann G & Misawa N (2002) Fungal carotenoids. In *The Mycota X Industrial Applications* (Osiewacz HD ed.), pp. 247–262. Springer Verlag, Berlin Heidelberg.
5 Avalos J & Cerdá-Olmedo E (2004) Fungal carotenoid production. In *Handbook of Fungal Biotechnology* (Arora DK ed.), pp. 367–378. Marcel Dekker, New York.

6 Avalos J, Cerdá-Olmedo E, Reyes F & Barrero AF (2007) Gibberellins and other metabolites of *Fusarium fujikuroi* and related fungi. *Curr Org Chem* **11**, 721–737.

7 Zalokar M (1957) Isolation of an acidic pigment in *Neurospora*. *Arch Biochem Biophys* **70**, 568–571.

8 Linnemannstöns P, Prado MM, Fernandez-Martin R, Tudzynski B & Avalos J (2002) A carotenoid biosynthesis gene cluster in *Fusarium fujikuroi*: the genes *carB* and *carRA*. *Mol Genet Genomics* **267**, 593–602.

9 Fernández-Martín R, Cerdá-Olmedo E & Avalos J (2000) Homologous recombination and allele replacement in transformants of *Fusarium fujikuroi*. *Mol Gen Genet* **263**, 838–845.

10 Prado-Cabrero A, Schaub P, Díaz-Sánchez V, Estrada AF, Al-Babili S & Avalos J (2009) Deviation of the neurosporaxanthin pathway towards β-carotene biosynthesis in *Fusarium fujikuroi* by a point mutation in the phytoene desaturase gene. *FEBS J* **276**, 4582–4597.

11 Prado-Cabrero A, Estrada AF, Al-Babili S & Avalos J (2007) Identification and biochemical characterization of a novel carotenoid oxygenase: elucidation of the cleavage step in the *Fusarium* carotenoid pathway. *Mol Microbiol* **64**, 448–460.

12 Prado-Cabrero A, Scherzinger D, Avalos J & Al-Babili S (2007) Retinal biosynthesis in fungi: characterization of the carotenoid oxygenase CarX from *Fusarium fujikuroi*. *Eukaryot Cell* **6**, 650–657.

13 Prado MM, Prado-Cabrero A, Fernández-Martín R & Avalos J (2004) A gene of the opsin family in the carotenoid gene cluster of *Fusarium fujikuroi*. *Curr Genet* **46**, 47–58.

14 Estrada AF & Avalos J (2009) Regulation and targeted mutation of *opsA*, coding for the NOP-1 opsin orthologue in *Fusarium fujikuroi*. *J Mol Biol* **387**, 59–73.

15 Avalos J & Cerdá-Olmedo E (1987) Carotenoid mutants of *Gibberella fujikuroi*. *Curr Genet* **25**, 1837–1841.

16 Avalos J & Schrott EL (1990) Photoinduction of carotenoid biosynthesis in *Gibberella fujikuroi*. *FEMS Microbiol Lett* **66**, 295–298.

17 Rodríguez-Ortiz R, Limón MC & Avalos J (2009) Regulation of carotenogenesis and secondary metabolism by nitrogen in wild-type *Fusarium fujikuroi* and carotenoid-overproducing mutants. *Appl Environ Microbiol* **75**, 405–413.

18 Thewes S, Prado-Cabrero A, Prado MM, Tudzynski B & Avalos J (2005) Characterization of a gene in the *car* cluster of *Fusarium fujikuroi* that codes for a protein of the carotenoid oxygenase family. *Mol Genet Genomics* **274**, 217–228.

19 Avalos J & Estrada AF (2010) Regulation by light in *Fusarium*. *Fungal Genet Biol* **47**, 930–938.

20 Schmidhauser TJ, Lauter FR, Russo VE & Yanofsky C (1990) Cloning, sequence, and photoregulation of *al-1*, a carotenoid biosynthetic gene of *Neurospora crassa*. *Mol Cell Biol* **10**, 5064–5070.

21 Schmidhauser TJ, Lauter FR, Schumacher M, Zhou W, Russo VE & Yanofsky C (1994) Characterization of *al-2*, the phytoene synthase gene of *Neurospora crassa*. Cloning, sequence analysis, and photoregulation. *J Biol Chem* **269**, 12060–12066.

22 Arrach N, Schmidhauser TJ & Avalos J (2002) Mutants of the carotene cyclase domain of *al-2* from *Neurospora crassa*. *Mol Genet Genomics* **266**, 914–921.

23 Saelices L, Youssar L, Holdermann I, Al-Babili S & Avalos J (2007) Identification of the gene responsible for torulene cleavage in the *Neurospora* carotenoid pathway. *Mol Genet Genomics* **278**, 527–537.

24 Estrada AF, Youssar L, Scherzinger D, Al-Babili S & Avalos J (2008) The *ylo-1* gene encodes an aldehyde dehydrogenase responsible for the last reaction in the *Neurospora* carotenoid pathway. *Mol Microbiol* **69**, 1207–1220.

25 Estrada AF, Maier D, Scherzinger D, Avalos J & Al-Babili S (2008) Novel apocarotenoid intermediates in *Neurospora crassa* mutants imply a new biosynthetic reaction sequence leading to neurosporaxanthin formation. *Fungal Genet Biol* **45**, 1497–1505.

26 Jin JM, Lee J & Lee YW (2010) Characterization of carotenoid biosynthetic genes in the ascomycete *Gibberella zeae*. *FEMS Microbiol Lett* **302**, 197–202.

27 Beutner S, Bloedorn B, Frixel S, Hernández Blanco I, Hoffmann T, Martin H-D, Mayer B, Noack P, Ruck C, Schmidt M *et al.* (2001) Quantitative assessment of antioxidant properties of natural colorants and phytochemicals: carotenoids, flavonoids, phenols and indigoids. The role of β-carotene in antioxidant functions. *J Sci Food Agric* **81**, 559–568.

28 Avalos J & Cerdá-Olmedo E (1986) Chemical modification of carotenogenesis in *Gibberella fujikuroi*. *Phytochemistry* **25**, 1837–1841.

29 Avalos J, Mackenzie A, Nelki DS & Bramley PM (1988) Terpenoid biosynthesis in cell-extracts of wild type and mutant strains of *Gibberella fujikuroi*. *Biochim Biophys Acta* **966**, 257–265.

30 Valadon LRG & Mummery RS (1977) Natural β-apo-4′-carotenoic acid methyl ester in the fungus *Verticillium agaricinum*. *Phytochemistry* **16**, 613–614.

31 Sakaki H, Kaneno H, Sumiya Y, Tsushima M, Miki W, Kishimoto N, Fujita T, Matsumoto S, Komemushi S & Sawabe A (2002) A new carotenoid glycosyl ester isolated from a marine microorganism, *Fusarium* strain T-1. *J Nat Prod* **65**, 1683–1684.

32 Valadon LRG, Osman M, Mummery RS, Jerebzoff-Quintin S & Jerebzoff S (1982) The effect of monochromatic radiation in the range 350 to 750 nm on the carotenogenesis in *Verticillium agaricinum*. *Physiol Plant* **56**, 199–203.

33 Leslie J (1991) Mating populations in *Gibberella fujikuroi* (*Fusarium* section Liseola). *Phytopathology* **81**, 1058–1060.

34 O'Donnell K, Cigelnik E & Niremberg HI (1998) Molecular systematics and phylogeography of the *Gibberella fujikuroi* species complex. *Mycologia* **90**, 465–493.
35 Avalos J, Casadesús J & Cerdá-Olmedo E (1985) *Gibberella fujikuroi* mutants obtained with UV radiation and N-methyl-N′-nitro-N-nitrosoguanidine. *Appl Environ Microbiol* **49**, 187–191.
36 Punt PJ, Oliver RP, Dingemanse MA, Pouwels PH & van den Hondel CA (1987) Transformation of Aspergillus based on the hygromycin B resistance marker from *Escherichia coli*. *Gene* **56**, 117–124.
37 Proctor RH, Hohn TM & McCormick SP (1997) Restoration of wild-type virulence to Tri5 disruption mutants of *Gibberella zeae* via gene reversion and mutant complementation. *Microbiology* **143**, 2583–2591.
38 Sambrook J & Russell DW (2001) *Molecular Cloning: a Laboratory Manual*. Cold Spring Harbor Laboratory Press, New York.
39 Thompson JD, Gibson TJ, Plewniak F, Jeanmougin F & Higgins DG (1997) The ClustalX windows interface: flexible strategies for multiple sequence alignment aided by quality analysis tools. *Nucleic Acids Res* **24**, 4876–4882.
40 Schultz J, Milpetz F, Bork P & Ponting CP (1998) SMART, a simple modular architecture research tool: identification of signaling domains. *Proc Natl Acad Sci USA* **95**, 5857–5864.

## Supporting information

The following supplementary material is available:
**Fig. S1.** High-resolution display of the HPLC elution profiles for SF134 and T3 shown in Fig. 7C between 45 and 50 min.

This supplementary material can be found in the online version of this article.

Please note: As a service to our authors and readers, this journal provides supporting information supplied by the authors. Such materials are peer-reviewed and may be re-organized for online delivery, but are not copy-edited or typeset. Technical support issues arising from supporting information (other than missing files) should be addressed to the authors.